Design of Implantable Microstrip Antenna for Communication With Medical Implants

Pichitpong Soontornpipit, Cynthia M. Furse, *Senior, Member*, and You Chung Chung, *Senior, Member*

***Abstract*—The objective of this paper is to design a microstrip patch antenna for communication with medical implants in the 402–405-MHz Medical Implant Communications Services band. Microstrip antenna design parameters are evaluated using the finite-difference time-domain method, and are compared to measured results. The effects of shape, length, size, location of feed point and ground point, substrate and superstrate materials, and their thicknesses are evaluated. An extensive study of the performance of the antennas to changes in these parameters was undertaken. The results of this paper provide guidance in the design of implantable microstrip antennas.**

***Index Terms*—Biocompatible antenna, Medical Implant Communications Services (MICS), microstrip, pacemaker antenna, wireless communication.**

I. Introduction

TRADITIONAL wireless communication techniques for air-to-air communication are improving and expanding at a phenomenal rate. Less traditional wireless communication systems may include air-to-subsurface or subsurface-to-subsurface transmission paths where the antennas are "embedded" in lossy material. Designing antennas for embedded applications is extremely challenging because of reduced antenna efficiency, impact of the environment on the antenna, the need to reduce antenna size, and the very strong effect of multipath losses. In addition to the current needs for embedded antennas, the expansion of microelectromechanical systems (MEMS) and wireless communication systems, which are expected to play a dominant role in next-generation technologies, will add dramatically to the applications for embedded antennas. Ultra-small devices (e.g., small enough to be injected into a human vein) and the desire to communicate with them, will inevitably lead to the need for miniaturized antennas embedded in lossy environments. This paper provides a better understanding of microstrip antennas embedded in lossy environments. The examples and sizes are typical of those that could be used for a cardiac pacemaker or similar-sized implantable device, but the observations and trends can be scaled to smaller devices and higher frequencies as needed.

A general theory of embedded antennas demonstrates their unique constraints and design considerations. Coaxial antennas, wire antennas, and arrays embedded in various lossy materials have been previously studied. Complete analytical solutions are available for cylindrical wire antennas with multilayer uniform insulation [1], and insulated antennas embedded in sand [2]. Numerical solutions are available for single antennas and arrays with nonuniform insulation embedded in nonuniform regions [3]–[5]. The use of nonuniform insulation was shown to improve the uniformity of the radiation from embedded antennas, a method that is extended to microstrip antennas in this paper. The insulation thickness was increased where the current density on the antenna was the highest, thereby reducing the coupling to the body and guiding the currents to utilize the full length of the antenna.

Embedded microstrip antennas have been used for several sensory applications including sensors for dielectric property measurement [6], [7], sensing the presence of a dielectric object [8], moisture measurement [9], and geophysical well logging [10]–[12]. Embedded microstrip antennas have been used therapeutically for a number of applications including cardiac ablation [13], [14], balloon angioplasty [15], and cancer treatment using hyperthermia [15]–[19]. Designers of antennas for sensing or therapy capitalize on some of the very problems that plague embedded antennas for communication—antennas are inherently sensitive to their environment (thus becoming good sensors), and inherently deposit large amounts of power in the near field of the antenna, particularly when it is embedded in lossy material, thus becoming good therapeutic tools. These are positive characteristics for sensing or therapy and negative characteristics for communication.

Nevertheless, several types of antennas have been used or proposed for a variety of embedded wireless communication applications. Inductive antennas (coils of wire around a dielectric or ferrite core) have been successfully used for biomedical telemetry [20]–[23], although data rates are low, and size/weight and biocompatibility issues plague the coil-wound devices. For cardiac telemetry, a dipole [24] and microstrip [25] embedded in the shoulder were analyzed using the finite-difference time-domain (FDTD) method.

The objective of this paper is to evaluate microstrip configurations for potential use for communication with medical implant devices. Microstrip designs were chosen because of their huge flexibility in design, conformability, and shape. Methods to reduce the size of the antenna by adding ground pins [thus converting the antenna to a shaped planar inverted F antenna (PIFA)], using high dielectric substrate materials, and spiraling the conductor shape (planar helix) are applied. Both uniform and nonuniform superstrate materials are evaluated.

The antennas are designed to operate in the 402–405-MHz band approved by the Federal Communication Commission (FCC) for Medical Implant Communications

Manuscript received September 4, 2003; revised January 27, 2004. This work was supported by the National Science Foundation under Grant 0080559.

The authors are with the Department of Electrical and Computer Engineering, University of Utah, Salt Lake City, UT 84112 USA (e-mail: youchung@ieee.org; cfurse@ece.utah.edu).

Digital Object Identifier 10.1109/TMTT.2004.831976

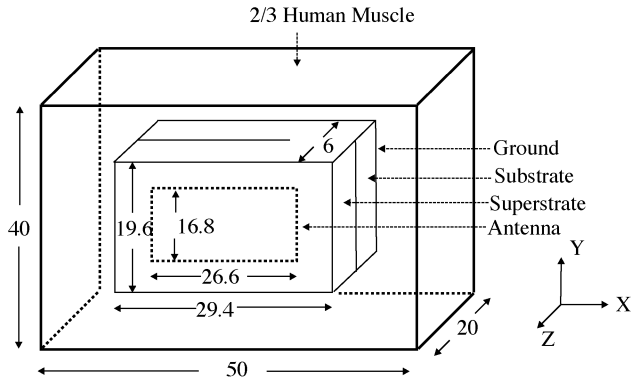

Fig. 1. Simulation model (in millimeters).

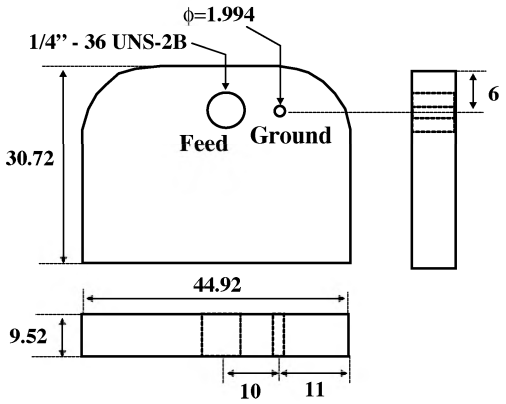

Fig. 2. Typical cardiac pacemaker battery pack size (in millimeters).

Services (MICS) [26], [27]. The simulation model is shown in Fig. 1, and the cardiac pacemaker battery pack (44.92 mm × 30.72 mm × 10 mm) used for prototyping is shown in Fig. 2. The antenna needs to be small enough (less than 34 mm × 24 mm) to fit on the surface of the battery pack, and this titanium battery pack serves as a finite ground plane for the antenna. The size of implants is continually shrinking so even smaller antennas will be needed in the future. The different antenna parameters are studied in free space, a homogenous block of muscle, and a realistic human shoulder model. A selected sample of these antennas was prototyped and tested in a simulated tissue material [28] on an HP8510C network analyzer.

II. Method of Analysis and Evaluation

The FDTD method was used for the simulation of microstrip antennas, as it has been used extensively for bioelectromagnetic simulations [29]–[31]. The general features of the current algorithm are as follows. The grid size is $\Delta x = \Delta y = \Delta z = 1$ mm, and the Mur absorbing boundaries are ten cells away from the antenna model. The superstrate is silicon ($\varepsilon_r = 3.1$, $\tan\delta = 0.0025$, and thickness $= 3$ mm). This is a commonly used biocompatible material with low electrical loss. Three biocompatible substrate materials are evaluated:

TABLE I
Effective Electrical Parameters of Different Substrates and Superstrates (Power is Given at 1 m When Max 1-g SAR = 1.6 W/kg)

	Substrate			Superstrate Parameters (substrate is Macor)		
	Teflon	Macor	Alumina			
ε_r	2.1	6.1	9.4	3.1	6.2	9.3
ε_{r_eff}	2.28	5.54	8.24	5.54	6.12	6.69
λ_{eff} (m)	0.115	0.179	0.218	0.115	0.188	0.197
Power (dBw)	-29.51	-31.60	-18.69	-31.60	-10.97	-6.28
Eff. (%)	4.16	21.37	35.18	21.37	9.62	6.36

Macor,[1] Teflon,[2] and Ceramic Alumina.[3] Properties of these substrates are given in Table I. Unless otherwise stated, the substrate is Macor throughout this paper. The antenna is embedded (centered) in a 50 × 40 × 20 mm^3 block of 2/3 human muscle ($\varepsilon_r = 42.807$ and $\sigma = 0.6463$ S/m), which is commonly used to represent average body properties. The electrical properties given are 2/3 those of pure muscle [32].

III. Parametric Study

In order to understand the performance of a microstrip antenna when implanted in a lossy material, a complete study of the effect of each parameter was undertaken.

A. Effect of Shape

In this test, two different shapes, spiral and serpentine, were simulated in order to compare their resonant frequencies [33]. The spiral antenna and serpentine antenna are identical in all ways (width = 2.8 mm and total length = 98 mm, where A = 7 mm, B = 8.4 mm, C = 7.7 mm, and D = 4.9 mm), except for how the antenna trace is placed on the board, as shown in Fig. 3. The $|E|$-field plots of the spiral and serpentine antennas are shown in Fig. 4. The main difference between these antennas is that the serpentine antenna has a higher resonant frequency for the same physical length, as shown in Fig. 5. The radiation patterns at the resonant frequency (402 and 475 MHz for spiral and serpentine antennas, respectively) in the 2/3 muscle block are shown in Fig. 6. From the distribution of magnitude of the electric field of these two antennas, shown in Fig. 4, it seems that the spiral antenna has strong coupling only at the center of the antenna, but the serpentine antenna also has coupling to adjacent arms [34]. This makes the serpentine antenna electrically shorter than the spiral antenna and, therefore, gives it a higher resonant frequency. Not surprisingly, the relative performance of the two antennas is also very similar, whether in air or 2/3 muscle. The

[1]Accuratus Ceramic Corporation, Macor Machinable Glass Ceramic (MGC), Washington, NJ. [Online]. Available: http://www.accuratus.com/Macor.htm, Nov. 2000.

[2]Dupont, "Comparison of different DuPont fluoropolymers." Willmington, DE. [Online]. Available: http://www.dupont.com/teflon.html, Dec. 2000.

[3]Omegaslate Ltd., Kidderminster, U.K. Omegaslate Ware Resistance Engineers. [Online]. Available: http://www.omegaslate.com/producti.html, Nov. 2000.

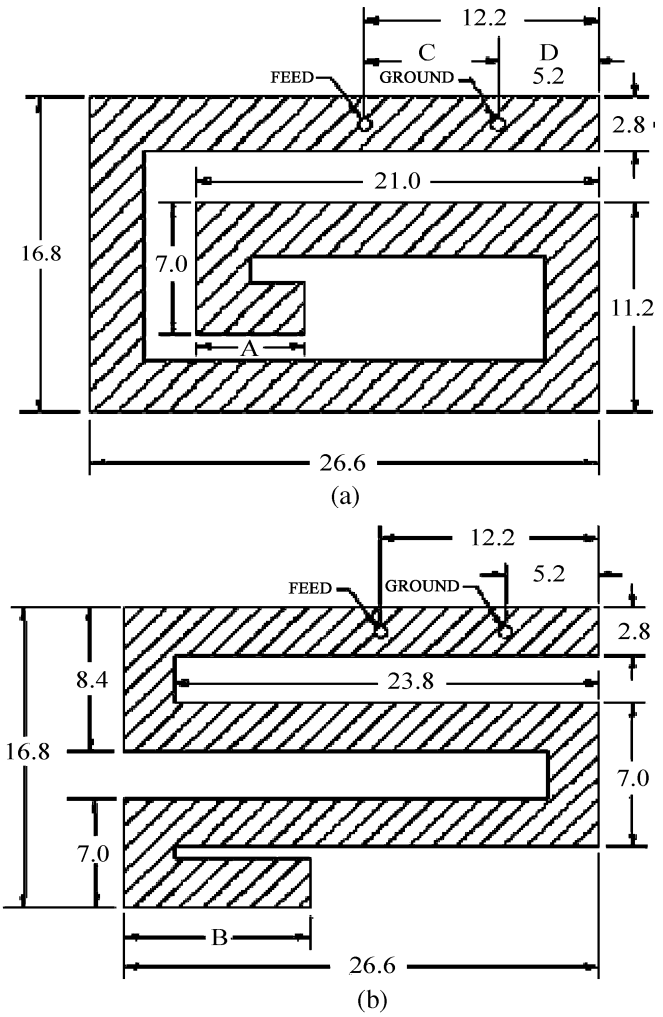

Fig. 3. (a) Spiral and (b) serpentine antennas (in millimeters). The antennas are in the x–y plane. The serpentine antenna (in millimeters) in the x–y plane.

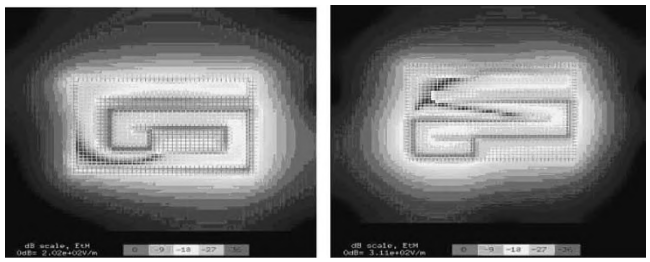

Fig. 4. $|E|$-field plots of the antennas.

radiated powers at 1 m for a fixed maximum 1-g specific absorption rate (SAR) of 1.6 W/kg for spiral and serpentine antennas in a 2/3 muscle block are -21 and -25 dBW, respectively. The spiral antenna radiates slightly better than the serpentine antenna, probably because of the more distributed current distribution, however, both would be reasonable for short-range wireless links. The 1-g SAR of 1.6 W/kg was used to limit the input power and, hence, the output power.

B. Effect of Length

To determine the effect of antenna length, the lengths of the spiral antenna arms A and serpentine arms B, shown in Fig. 3,

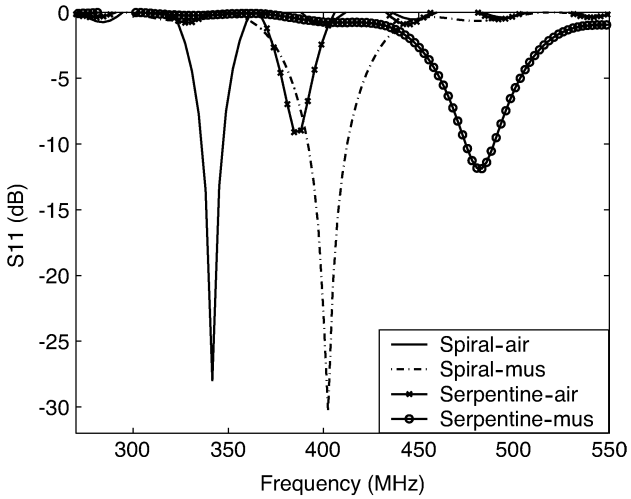

Fig. 5. Comparison between $|S_{11}|$ of spiral and serpentine antennas in 2/3 muscle and air. The serpentine antenna is electrically shorter than the spiral antenna and, therefore, has a higher resonant frequency.

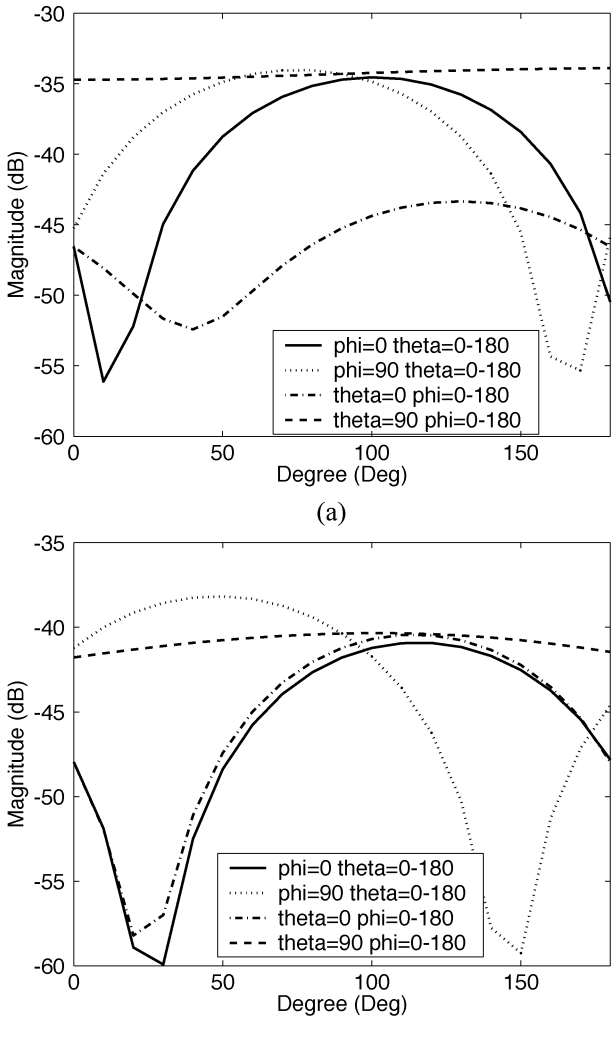

Fig. 6. Gain pattern (in decibels relative to isotropic) of: (a) spiral and (b) serpentine antennas.

were changed, and the antenna was simulated in a block of 2/3 human muscle. As expected, and as shown in Fig. 7, longer antennas have lower resonant frequencies. In addition, the antenna

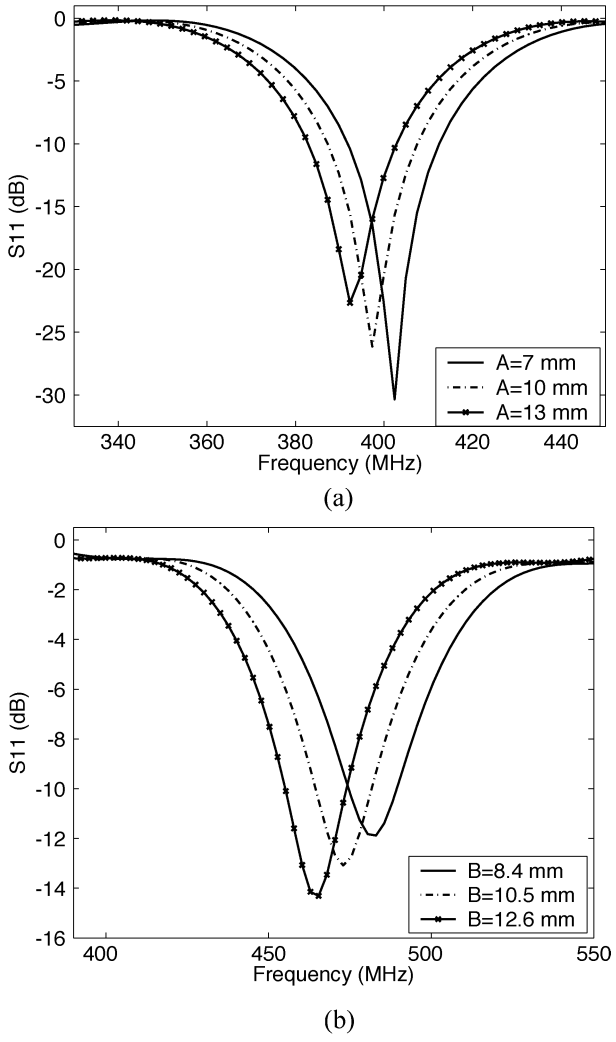

Fig. 7. Magnitude of the reflection coefficient as a function of increasing the length of the: (a) spiral arm A and (b) serpentine arm B.

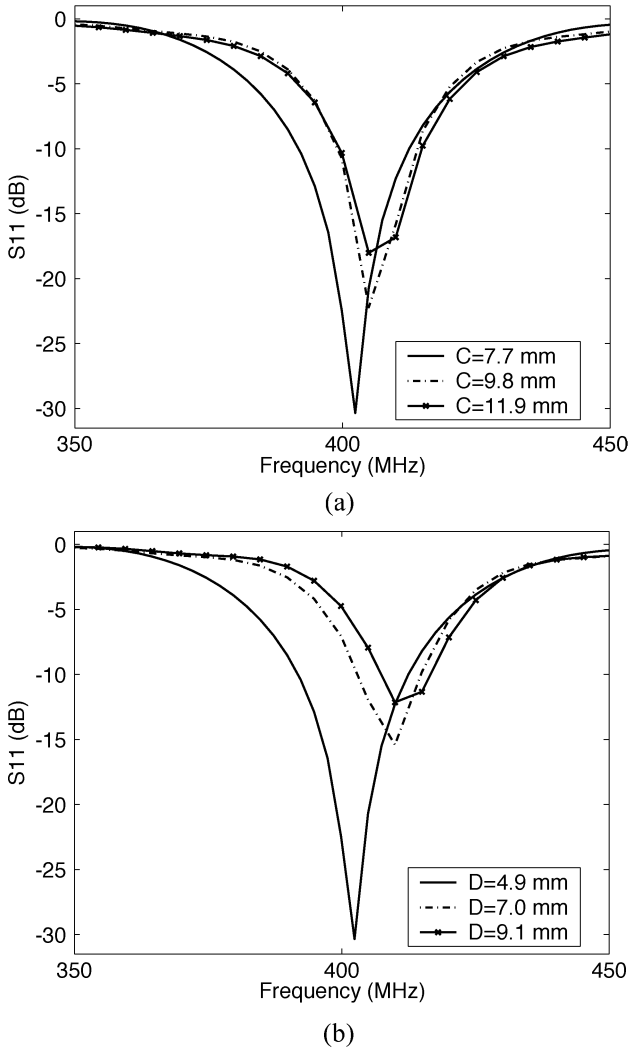

Fig. 8. Comparison between $|S_{11}|$ of spiral antennas as a function of: (a) feed point location C (when D is 4.9 mm) and (b) ground point location D (when C is 7.7 mm).

matching changes, but as we will see in the following sections, this can be tuned by adjusting other antenna parameters. Increasing the length of the antenna changes the radiated power at 1 m by less than 0.4 dB.

C. Effect of Feed and Ground Point Locations

The antenna is fed with a standard coaxial probe feed, and the location of the feed would be expected to affect the tuning of the antenna. The spiral design can be thought of as a modified monopole antenna, twisted up to reduce the size, and the ground pin acts somewhat as a ground plane on a monopole antenna, nearly doubling its electrical size. Therefore, adding a ground pin can reduce the required size of the antenna for a given frequency. This antenna is then similar to PIFA antenna designs, although the "plane" of the antenna is shaped like a serpentine or spiral.

The effects of the feed and extra ground point locations were evaluated by changing the lengths of C and D, shown in Fig. 3(a), for the spiral antenna. First, the ground location was fixed at $\mathrm{D} = 4.9$ mm, and the feed was moved, and then the feed was fixed at $\mathrm{C} = 7.7$ mm, and the ground was moved. As shown in Fig. 8, the locations of the feed and ground point impact the antenna matching, but have little effect on the resonant frequency. In addition, having a slightly longer distance between feed and ground increases the bandwidth slightly (in this case, up to 0.5 MHz).

D. Effect of Substrate and Superstrate Materials

The choice of substrate and superstrate materials is critical in the design of long-term biocompatible antennas. A comparison of three commercially available substrate materials (Macor, Teflon, and ceramic aluminum), each 3-mm thick, is shown in Fig. 9(a). The effect of varying the electrical permittivity of the superstrate is shown in Fig. 9(b). As expected, higher permittivity results in lower resonant frequency because the effective wavelength is shorter. The effective parameters of the substrate and superstrate are calculated [35]–[37], and the results are shown in Table I. Different values of the superstrate were compared to determine if doping the superstrate would be valuable, as analyzed in Section III-F.

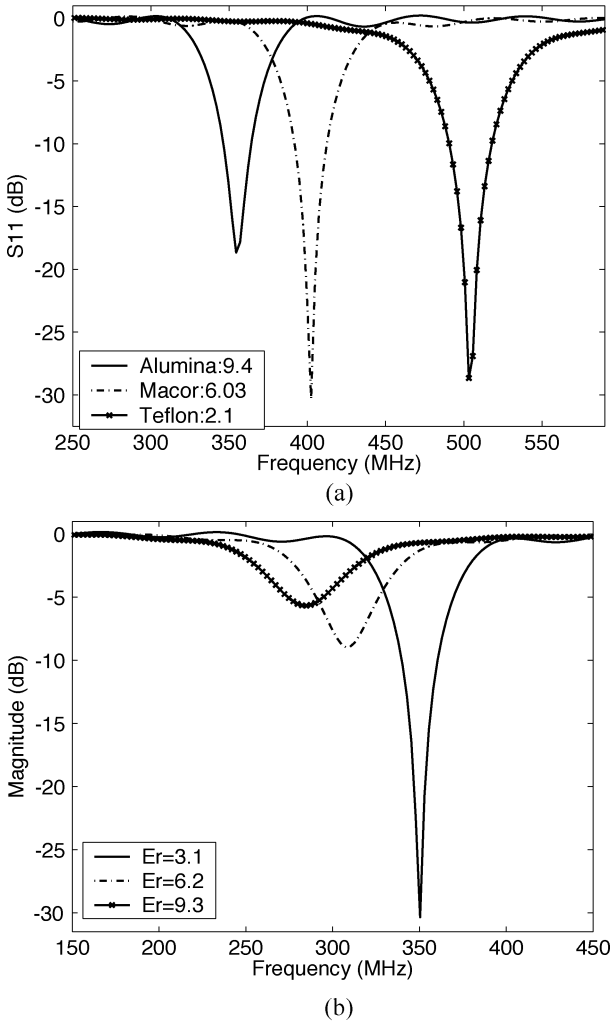

Fig. 9. Comparison between $|S_{11}|$ of spiral antennas as a function of: ; (a) substrate materials and (b) superstrate materials.

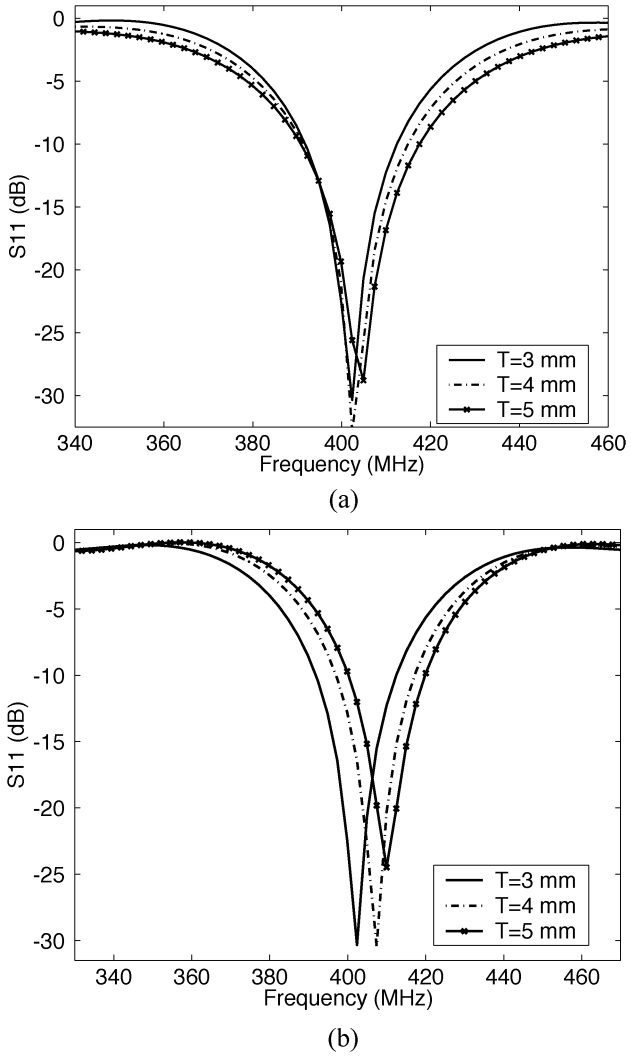

Fig. 10. Comparison between $|S_{11}|$ of spiral antennas as a function of: (a) substrate thickness and (b) superstrate thickness.

E. Effect of Substrate and Superstrate Thickness

When the thickness of the substrate is increased, the effective dielectric constant is also increased, and the antenna will appear electrically longer and, hence, have a slightly lower resonant frequency. This can be seen in Fig. 10. First, the superstrate thickness was fixed at 3 mm, and the substrate thickness was increased, and then the substrate thickness was fixed at 3 mm, and the superstrate thickness was increased. As we can see in Fig. 10, when the superstrate thickness is increased, the resonant frequency is decreased, because the thicker superstrate actually reduces the effective permittivity by insulating the antenna from the higher dielectric body material. There is minimal change when the substrate thickness is changed.

Materials with high dielectric constant will enable smaller antennas, however, they tend to also have higher loss due to the surface wave and, therefore, poor efficiency. The high dielectric of the human body above the antenna effectively reduces the wavelength near the antenna and, hence, physical size, though, of course, the body is highly lossy, and absorbs much of the signal. The superstrate material (which also should be low loss) reduces the power deposited in the body very near the antenna. This is very important to maintain the SAR below the FCC-approved limit [26] of 1.6 W/kg. In effect, the superstrate is preventing the body from shorting out the antenna.

F. Effect of Nonuniform Superstrate

As we can observe from the steady-state plots of electric-field magnitude, shown in Fig. 4, more concentration of current is seen on the inner arm of the spiral antenna where the current reflects off the end of the antenna and the outermost arm, which is closest to the feed and ground points.

One method of reducing the total size of the antenna is to place superstrate material only over the areas with high current. This is shown in Fig. 11(a). The results are shown in Fig. 12(a), and the radiated powers at 1 m for a maximum 1-g SAR of 1.6 W/kg are -29.5 and -30.4 dBW, respectively. Very little change is observed if the antenna is built as a concave antenna, with a flat superstrate, or if the antenna is flat and the superstrate is convex, as shown. The concave antenna would have the smallest possible total thickness if space can be spared for the concavity.

The effect of nonuniform electrical properties of the superstrate is also of interest. A possible way of improving the

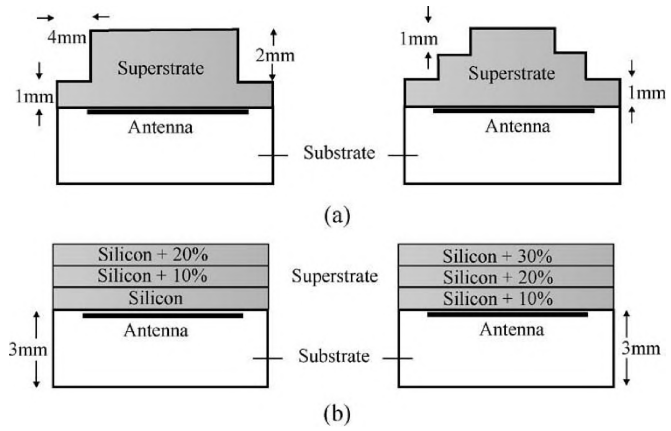

Fig. 11. Structure of the antenna in the Z–X-plane as a function of: (a) saline in the material and (b) soaking superstrate layers.

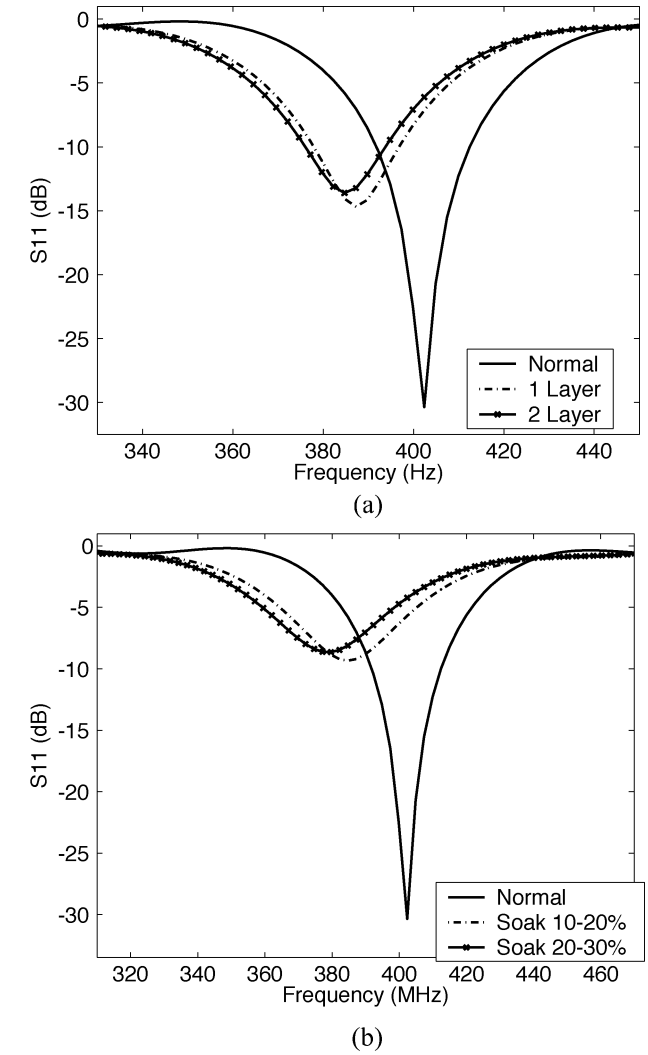

Fig. 12. Comparison between $|S_{11}|$ of spiral antennas as a function of a: (a) convex superstrate and (b) superstrate partially permeated by body fluid.

matching between the superstrate and body might be to allow the body fluid to permeate the superstrate [37]. In order to test this possibility, the percentages of body fluids that might be allowed to permeate the superstrate were controlled by either saline addition or holes in the material, as shown in Fig. 11(b).

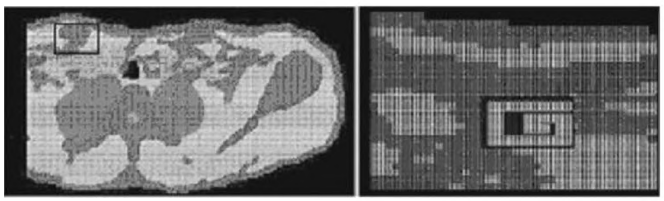

Fig. 13. X—Y section of realistic shoulder (370 mm × 170 mm) used in the design.

TABLE II
PERMITTIVITIES AND CONDUCTIVITIES FOR TISSUES OF THE REALISTIC SHOULDER AT 433 MHz FROM [32]

Material	ε_r	σ
Fat	5.028	0.04502 S/m
Bone	17.35	0.16725 S/m
Cartilage	43.64	0.65 S/m
Skin	46.68	0.64 S/m
Nerve	35.7	0.5 S/m
Blood	57.29	1.72 S/m
Muscle	42.807	0.64633 S/m
Lung	21.58	0.3561 S/m

In this case, the outermost superstrate was divided into three layers and assumed to be partially permeated by body fluid, with percentages decreasing from the body to the antenna, as shown in Fig. 11(b). Each layer is 1-mm thick. The dielectric properties of the layer with 10% body fluid are assumed to be $\varepsilon r = 4.2$, $\sigma = 0.0646$ S/m, with 20% body fluid, $\varepsilon r = 8.4$, $\sigma = 0.129$ S/m, and with 30% body fluid, $\varepsilon r = 12.6$, $\sigma = 0.19$ S/m. The effect results of the nonuniform electrical properties of the superstrate are shown in Fig. 12(b), and the radiated powers at 1 m for a maximum 1-g SAR of 1.6 W/kg are −30.1 and −30.6 dBW, respectively.

IV. Analysis of the Antenna in the Realistic Shoulder

In the above sections, the antennas were analyzed in a block of 2/3 muscle (50 mm × 40 mm × 20 mm). Here, they are analyzed in a more realistic model of the human shoulder in order to determine if the more realistic model (390 mm × 180 mm × 190 mm) is needed for the design of the antenna, shown in Fig. 13. This model, derived from the University of Utah man model [38] has 31 different tissues. The dielectric permittivities and conductivities of tissues are shown in Table II for 433 MHz [32]. A comparison of the antennas in a block of 2/3 human muscle and in the shoulder is given in Fig. 14. Some shift in frequency is indeed observed. The maximum 1-g SAR is 0.06, 0.15, and 0.29 W/kg for an input voltage of 1 kV/m for the 2/3 muscle, realistic shoulder, and TK-151, respectively. It was determined that the exact location of the antenna in the realistic shoulder has a sizeable effect on these parameters, as expected. The best practice for antenna design would, therefore, be to do an approximate design with the 2/3 muscle block where the simulation runs quicker, and use detailed modeling only on the final design.

V. Prototype and Measurement Results

In order to verify the simulation results, prototypes of the spiral antenna were built from Macor substrate, as shown

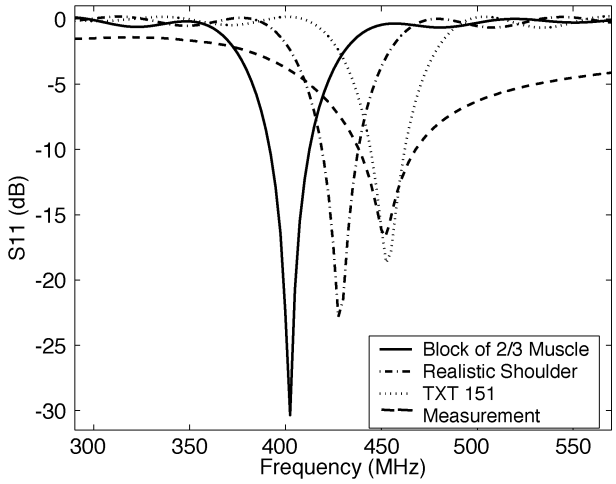

Fig. 14. Comparison between $|S_{11}|$ of spiral antennas in a block of 2/3 human muscle, a realistic shoulder model, TX-151, and a tissue simulant material.

in Fig. 3(a). Household silicon (same dielectric properties as medical-grade silicon) was used for the superstrate. The magnitude of the reflection coefficient was measured with an HP8510C network analyzer. The tissue simulant material made from TX-151 powder, mixed with sugar, salt, and water was used as the test material, which has a dielectric permittivity of 48.943 and a conductivity of 0.7099 S/m [32], [39]. The comparison between simulation and measurement results is shown in Fig. 14. The measurements and simulations are within the expected range of the modeling, considering the differences in the dielectric properties of materials (2/3 muscle, shoulder, and TX-151).

VI. Conclusion

Spiral and serpentine microstrip antennas that can be used for communication with medical devices have been analyzed in the 402–405-MHz ranges. Based on this research, several observations were made. Both spiral and serpentine designs were found to be effective radiators for communication with medical implants in the 402–405-MHz MICS band. The spiral design was the smaller of the two designs and both were significantly smaller than a traditional rectangular patch. For optimal design, a biocompatible substrate and superstrate should have the largest possible ε_r, while having low conductivity, and thicker substrate and superstrate are better than thin. The best design can be found by first choosing the substrate and superstrate materials, then optimizing the length to provide approximately the correct resonant frequency. Finally, the antenna should be tuned by varying the location of the feed point with the ground point fixed very near one end of the antenna. The current distribution can then be observed, and an overall thinner design can be produced by using a superstrate that is thicker where the current density is high. It was also noted that while an homogenous model is sufficient for the basic design of the antenna, a more realistic model of the shoulder is needed to provide accurate 1-g SAR results, and to tune the final antenna design.

References

[1] O. Gandhi, G. Lazzi, and C. M. Furse, "Electromagnetic absorption in the human head and neck for mobile telephones at 835 and 1900 MHz," *IEEE Trans. Microwave Theory Tech.*, vol. 44, pp. 1884–1897, Oct. 1996.

[2] C. Furse and O. P. Gandhi, "Calculation of electric fields and currents induced in a millimeter-resolution human model at 60 Hz using the FDTD method," *Bioelectromagnetics*, vol. 19, no. 5, pp. 293–299, 1998.

[3] R. Johnson, J. R. James, J. W. Hand, J. W. Hopewell, P. Dunlop, and R. Dickinson, "New low-profile applicators for local heating of tissues," *IEEE Trans. Biomed. Eng.*, vol. BME-31, pp. 28–36, Jan. 1984.

[4] I. J. Bahl, S. Stuchly, J. Lagendijk, and M. Stuchly, "Microstrip loop applicators for medical applications," *IEEE Trans. Microwave Theory Tech.*, vol. MTT-30, pp. 1090–1093, July 1982.

[5] G. Lazzi, S. S. Pattnaik, C. M. Furse, and O. P. Gandhi, "Comparison of FDTD-computed and measured radiation patterns of commercial mobile telephones in presence of the human head," *IEEE Trans. Antennas Propagat.*, vol. 46, pp. 943–944, June 1998.

[6] C. Deffendol and C. Furse, "Microstrip antennas for dielectric property measurement," in *IEEE AP/URSI Int. Symp. Dig.*, vol. 3, Orlando, FL, July 1999, pp. 1954–1957.

[7] I. J. Bahl and S. S. Stuchly, "Analysis of a microstrip covered with a lossy dielectric," *IEEE Trans. Microwave Theory Tech.*, vol. MTT-28, pp. 104–109, Feb. 1980.

[8] C. M. Furse, "A meander antenna used as a human proximity sensor," Mission Res. Inc., Logan, UT, Final Rep., July 1998.

[9] N. Madan, "Imbedded antennas for the measurement of electrical properties of materials," M.S. thesis, Dept. Elect. Comput. Eng., Utah State Univ., Logan, UT, 2001.

[10] D. Johnson, E. Cherkaev, C. Furse, and A. Tripp, "Cross-borehole delineation of a conductive ore deposit—Experimental design," *Geophysics*, vol. 66, no. 3, pp. 824–835, 2001.

[11] D. Johnson, C. Furse, and A. Tripp, "FDTD modeling and validation of EM survey tools," *Microwave Opt. Technol. Lett.*, vol. 34, no. 6, pp. 427–429, 2002.

[12] P. S. Debroux, "Modeling of the electromagnetic response of geophysical targets using the (FDTD) method," *Geophys. Prospecting*, vol. 44, no. 3, pp. 457–468, 1996.

[13] R. D. Nevels, D. Arndt, J. Carl, G. Raffoul, and A. Pacifico, "Microwave antenna design for myocardial tissue ablation applications," in *IEEE AP-S Int. Symp. Dig.*, vol. 3, Newport Beach, CA, June 1995, p. 1572.

[14] A. S. Manolis, P. J. Wang, and N. A. Estes, "Radio frequency catheter ablation for cardiac tachyarrhythmias," *Annu. Int. Med.*, vol. 121, no. 6, pp. 452–461, Sept. 1994.

[15] A. Rosen, "Microwave applications in cancer therapy, cardiology and measurement techniques: A short overview," *IEEE MTT-S Newslett.*, pp. 17–20, Fall 1990.

[16] A. Guy, J. F. Lehman, and J. B. Stonebridge, "Therapeutic applications of electromagnetic power," *Proc. IEEE*, vol. 62, pp. 55–75, Jan. 1974.

[17] M. F. Iskander, A. M. Tumeh, and C. M. Furse, "Evaluation and optimization of the EM characteristics of interstitial antennas for hyperthermia," *Int. J. Radiat., Oncol., Biol., Phys.*, vol. 18, no. 4, pp. 895–902, Apr. 1990.

[18] C. M. Furse and M. F. Iskander, "Three-dimensional electromagnetic power deposition in tumors using interstitial antenna arrays," *IEEE Trans. Biomed. Eng.*, vol. 36, pp. 977–986, Oct. 1989.

[19] P. C. Cherry and M. F. Iskander, "Calculations of heating patterns of an array of microwave interstitial antennas," *IEEE Trans. Biomed. Eng.*, vol. 40, pp. 771–779, Aug. 1993.

[20] W. G. Scanlon, N. E. Evans, and J. B. Burns, "FDTD analysis of closed-coupled 4–18 MHz radiating devices for human biotelemetry," *Phys. Med. Biol.*, vol. 44, no. 2, pp. 335–345, 1999.

[21] W. G. Scanlon, N. E. Evans, and Z. M. McCreesh, "RF performance of a 418 MHz radio telemeter packaged for human vaginal placement," *IEEE Trans. Biomed. Eng.*, vol. 44, pp. 427–430, May 1997.

[22] W. G. Scanlon, N. E. Evans, and J. B. Burns, "FDTD analysis of close-coupled 418 MHz radiating devices for human biotelemetry," *Phys. Med. Biol.*, vol. 44, no. 2, pp. 335–345, Feb. 1999.

[23] G. C. Crumley, N. E. Evans, J. B. Burns, and T. G. Trouton, "On the design and assessment of a 2.45 GHz radio telecommand system for remote patient monitoring," *Med. Eng. Phys.*, vol. 20, no. 10, pp. 750–755, Mar. 1999.

[24] J. Schuster and R. Luebbers, "An FDTD algorithm for transient propagation in biological tissue with a Cole–Cole dispersion relation," in *IEEE AP/URSI Int. Symp. Dig.*, vol. 4, June 1998, pp. 1988–1991.

[25] C. M. Furse, "Desing of an antenna for pacemaker communcation," *Microwaves RF*, vol. 39, no. 3, pp. 73–76, Mar. 2000.
[26] "FCC guidelines for evaluating the environmental effects of radio frequency radiation," FCC, Washington, DC, 1996.
[27] "Medical Implant Communications Service (MICS) federal register," *Rules and Regulations*, vol. 64, no. 240, pp. 69 926–69 934, Dec. 1999.
[28] S. Going and B. J. Mcleod, "Biocompatible materials for microstrip pacemaker antenna," Mech. Eng. Dept., Utah State Univ., Logan, UT, Senior Project, 2001.
[29] C. Furse, R. Mohan, A. Jakayar, S. Kharidehal, B. McCleod, S. Going, L. Griffiths, P. Soontornpipit, D. Flamm, J. Bailey, I. H. Budiman, and M. Hullinger, "A biocompatible antenna for communication with implantable medical devices," in *IEEE AP/URSI Int. Symp. Dig.*, June 2002, p. 131.
[30] I. J. Bahl, P. Bhartia, and S. S. Stuchly, "Design of microstrip antennas covered with a dielectric layer," *IEEE Trans. Antennas Propagat.*, vol. AP-30, pp. 314–318, Mar. 1982.
[31] S. Kharidehal, "Design and measurement of implantable antennas," M.S. thesis, Dept. Elect. Comput. Eng., Utah State Univ., Logan, UT, 2002.
[32] "Occupational and environmental health directorate," Radiofreq. Rad. Div., Brooks Air Force Base, Brooks AFB, TX, June 1996.
[33] M. Ali, M. Okoniewski, and S. S. Stuchly, "Study of a printed meander antenna using the FDTD method," *Microwave Opt. Technol. Lett.*, vol. 37, no. 6, pp. 440–444, June 2003.
[34] P. Soontornpipit, "Design of Implantable antennas for communication with medical implants," M.S. thesis, Dept. Elect. Comput. Eng., Utah State Univ., Logan, UT, 2002.
[35] P. Buntschuh and P. Charles, "High directivity microstrip couplers using dielectric overlays," in *IEEE MTT-S Int. Microwave Symp. Dig.*, 1975, pp. 125–127.
[36] K. Chang and J. Klein, "Dielectrically shielded microstrip (DSM) lines," *Electron. Lett.*, vol. 23, no. 10, pp. 535–537, May 1987.
[37] J. Callarotti, C. Roberto, and A. Gallo, "On the solution of a microstripline with two dielectrics," *IEEE Trans. Microwave Theory Tech.*, vol. MTT-32, pp. 333–339, Apr. 1984.
[38] O. P. Gandhi and C. M. Furse, "Millimeter-resolution MRI-based models of the human body for electromagnetic dosimetry from ELF to microwave frequency," in *Proc. Int. Radiological Protection Board Workshop*, Chilton, U.K., July 1995, pp. 24–31.
[39] D. Flamm, "Biocompatible materials for microstrip pacemaker antenna," Elect. Comput. Eng. Dept., Utah State Univ., Logan, UT, Senior Project, 2002.

Pichitpong Soontornpipit received the B.S. degree from the Mahanakorn University of Technology, Bangkok, Thailand, in 1997, the M.S. degree from Utah State University, Logan, in 2001, and is currently working toward the Ph.D. degree in electrical and computer engineering at the University of Utah, Salt Lake City.

He is currently with The Self Organizing Intelligent System and Center of Excellent for Smart Sensors, University of Utah. His current research involves development of antennas, optimized antennas, and genetic algorithms.

Cynthia M. Furse (S'85–M'87–SM'99) received the Ph.D. degree from the University of Utah, Salt Lake City, in 1994.

She is currently the Director of the Center of Excellence for Smart Sensors, University of Utah, Salt Lake City, and Associate Professor with the Electrical and Computer Engineering Department, University of Utah. The Center focuses on embedded sensors in complex environments, particularly sensors for anomalies in the human body and aging aircraft wiring. She directed the Utah "Smart Wiring" program, which is sponsored by NAVAIR and the U.S. Air Force (USAF) for the past six years. She teaches electromagnetics, wireless communication, computational electromagnetics, microwave engineering, and antenna design.

Dr. Furse is a National Science Foundation Computational and Information Sciences and Engineering Graduate Fellow, the IEEE Microwave Theory and Techniques Society (IEEE MTT-S) Graduate Fellow, and the President's Scholar at the University of Utah. She is the chair of the IEEE Antennas and Propagation Society (IEEE AP-S) Education Committee and an associate editor of the IEEE TRANSACTIONS ON ANTENNAS AND PROPAGATION. She was the 2000 Professor of the Year in the College of Engineering, Utah State University and the 2002 Faculty Employee, Utah State University.

You Chung Chung (S'94–A'95–M'00–SM'03) received the B.S. degree in electrical engineering from Inha University, Inchon, Korea, in 1990, and the M.S.E.E. and Ph.D. degrees from the University of Nevada at Reno (UNR), in 1994 and 1999, respectively.

He is currently a Research Assistant Professor of electrical and computer engineering with the University of Utah, Salt Lake City. He has been with the Center of Excellence for Smart Sensors and CSOIS, Utah State University. His research interests include computational electromagnetics, optimized antenna and array design, conformal and fractal antennas, smart wireless sensors, aging aircraft wire detection sensors, optimization techniques, electromagnetic (EM) design automation tool development, and genetic algorithms.

Dr. Chung was the recipient of the 1996 Outstanding Teaching Assistant Award presented by the UNR. He was also the recipient of a 1999 Outstanding Graduate Student Award. The National Science Foundation (NSF) sponsored his 1999 IEEE Antennas and Propagation (IEEE AP-S) paper presentation. In 2000, he was the recipient of the Third Student Paper Award presented by the International Scientific Radio Union (URSI) International Student Paper Competition.